JOURNAL OF MECHANICAL ENGINEERING AND SCIENCES (JMES)
ISSN: 2289-4659 e-ISSN: 2231-8380
VOL. 14, ISSUE 3, 7040 – 7048
DOI: https://doi.org/10.15282/jmes.14.3.2020.06.0551

ORIGINAL ARTICLE

Rotordynamics analysis of a single helical gear transmission system for high speed applications

Najeeb Ullah, C. Xi, T. Cong, and H. Yucheng

The State Key Laboratory of Mechanical Transmissions, Chongqing University, Chongqing 400030, China
Phone: +8613271956049

ABSTRACT – Since the non-linear dynamic response under various high-speed conditions can directly affect the life of gear transmission systems. In addition, the transmission error and dynamic mesh force play a key role in noise and harshness analysis of gear bearing coupled systems. So, in this piece of work, a 12 degree of freedom dynamic model is developed to probe the vibration response by using finite element method and taking into account the bearing and flexible shafts in the first part. Subsequently, some meshing gear characteristics such as dynamic and vibration acceleration response under different rotational speeds (1000-9000 rev/minute) were analyzed whereas critical speed appeared at 6500 rev/minute. Then, the stability analysis is performed to investigate the dynamics behind the critical speed by using MASTA. It was observed that natural frequency of 0.45 kHz for a fourth harmonic order is analogous to critical speed which further causes sudden elevation in both dynamic mesh force and transmission error.

ARTICLE HISTORY
Revised: 03rd Dec 2019
Accepted: 31st Mar 2020

KEYWORDS
Finite element method; gear transmission systems; stability analysis; critical speed; transmission error

INTRODUCTION

Single helical gears seem a suitable choice for many complex mechanical systems and are considered as more suited for mechanical drives in which each application could require a "unique" design for power and speed. For remote and offshore platforms, many researchers believe as they are simple and reliable means of adjustment in the field, though with a lower efficiency as compared to double helical gears. However, there is a cost to be paid in gaining a better efficiency, affecting operating values. Many studies have been done to understand and resolve the complexity of gear rotor dynamics. In the beginning, single tooth and tooth pair models were developed. For instance, the flexibility of the shaft and bearing were all neglected. The studies conducted by H. Nevzat and G. Blankenship [1,2] present an elaborative review for such models. One category of gear pair research is of primary importance as these non-linear models considers the gear pair including shaft and bearing dynamics [3-7]. The shaft flexibilities were presented from corresponding lumped springs to finite element interpretations in this study. The dynamic analysis of a linear model for helical geared system was investigated [8]. A proposition in [9] illustrates a dynamic model having ten degrees of freedom, which takes into account the shaft, bearing latitude, and the dynamic coupling among different kind of motions. A finite element methodology for the gearbox coupled with different speed shafts was presented which has the potential to apply to a vast range of both helical and spur geared systems.

The analysis reveals the manufacturing error of spur gear while the dynamic model of gear rotor and the non-linear vibrations were focused by using a one degree of freedom system for both perfect and imperfect gears [10]. The investigation conducted by W.Kim et.al [11] is about the dynamic impact of spur gear pairs caused by bearing deformation. In this study, behavior of damping and stiffness upon the dynamic responses is also analyzed. C. Kang et.al [12] investigated the dynamic response of gear rotor system fixed on viscoelastic supports by considering gear eccentricity, the finite element formulation with the excitation of transmission error and residual bow effect. Later on, study in [13] focused on exploring the mechanism of spur geared system along with spalling response on mesh stiffness and non-linear dynamic characteristics to analyze the failure factors of spalling vibration signals. While, a dynamic method in [14] considered the non-linear forced oscillations and vibration level of spur gear pair including the stability analysis with a third order polynomial function of dynamic transmission error (cubic nonlinearity). A finite element model of a spur gear pair with tip relief was developed using ANSYS software. While the most attention in this study was given to the impact of tip relief and amplitude fluctuation on vibration behavior of the system [15]. The dynamic analysis of gear rotor in [16] presented systems under time-periodic based motions and obtained the lateral and torsional behavior under transmission error and mass excitations in unbalanced state.

The lumped parameter gear model was developed to predict gear pair dynamics with varying time and frequency resolution using measured quasi-static transmission error [17]. A 12 DOF dynamic model is established in [18] by considering the gyroscopic effects and performed vibration-based tooth crack analysis. The rotor dynamics of double helical gear transmission system was taken into account in [19] proposed and shaft was treated as a Timoshenko beam finite element. Besides that, effects of mesh stiffness by considering non-linearity of backlash were studied using the Lagrange's equations [20]. Though bearing-rotor coupling dynamics was not focused numerically in [21]. But non-linear vibration was studied in a sliding rotor bearing system and the rotor speed up and speed down experiments were performed

*CORRESPONDING AUTHOR | Najeeb Ullah | najeeb.rr@gmail.com

which gives the apprehension of water film whirl and whip in the water lubricated sliding bearing. Later on, vibration signal analysis for energy harvester and gearbox diagnosis strategy were investigated [22,23].

Based on the aforementioned study, it is obvious that there is a rare work related to the nonlinear dynamic behavior of the single-helical gear set especially under different operating speed conditions. Hence, this study presents the rotor dynamics for a single-stage helical gear transmission system by considering bearing and flexible shafts in the model. A 12 degree of freedom gear mesh model is established and the equations of motion with bearings, shafts and gyroscopic effect are obtained. Each element is assembled by finite element method to establish full dynamic model of the coupled gear bearing system. Then, the impact of the behavioral response on the gear system under different speeds is studied by calculating some of the dynamic response characteristics as well as stability analysis.

FINITE ELEMENT APPROACH FOR SINGLE STAGE HELICAL GEAR REDUCTION

Figure 1 delineate a single-stage gear transmission system diagram, while the relevant parameters are given in Table 1 and 2. The proposed system comprises of two shafts, a pair of meshing gears and two pairs of bearings. Input shaft is mounted on motor and output shaft is connected with the load. Finite element model is shown in Figure 3, where by taking into account the input and output shaft for the reference axis, each shaft is divided into 6 sections. The bearings are replaced by massless springs and dampers, whose forces are assumed to be at the bearing mid-point, the four bearings acting at four nodes. Since the actual gear is a stepped gear, the middle section of the central section is assumed to be a shaft, and the same part as the tooth width is assumed to be rigid rotor acting on the shaft. The meshing effect of meshing gear pairs is expressed in terms of stiffness. A total of 12 nodes are needed for modelling. Each node has six degrees of freedom, consisting of three translational and three rotational degrees of freedom. So finally, there will be 72 DOF for overall system.

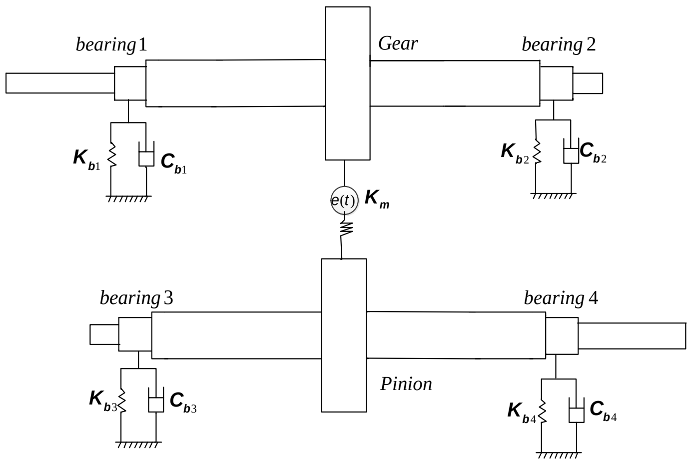

Figure 1. Single stage structure for gear transmission system

The gear is regarded as concentrated mass and we used lumped mass method to build the dynamic model of the gear pairs initially. Then, the stiffness, mass and damping matrix of each dynamic equation are assembled according to the finite element method. In this way, we developed the dynamic model of the whole gear transmission system. Generally, the number of nodes and units are determined by the actual setup and calculation accuracy requirements of the gear transmission structure.

Dynamic Modeling of Gear Mesh Unit

A 12 degree of freedom gear mesh dynamic model is developed using Lagrange's approach. Gear and pinion are considered as rigid elements with 6 degrees in translational and rotational directions $x_i, y_i, z_i, \theta_{xi}, \theta_{yi}, \theta_{zi}$ where $(i = p, g)$ stands for gear and pinion as shown in Figure2. O_p and O_g are gear pair central points in x, y and z directions whereas β, α are helix angle and pressure angle respectively. The system's generalized coordinates can be expressed as:

$$q = \{x_p, y_p, z_p, \theta_{px}, \theta_{py}, \theta_{pz}, x_g, y_g, z_g, \theta_{gx}, \theta_{gy}, \theta_{gz}\}^T \quad (1)$$

In addition, following key assumptions were made in building dynamic model:

1. Shaft mass and inertia are united at the gears;
2. Backlash is not considered in this model, thus there is no tooth separation.

Based on Lagrange's method, the dynamic equations for the gear meshing element model can be written as:

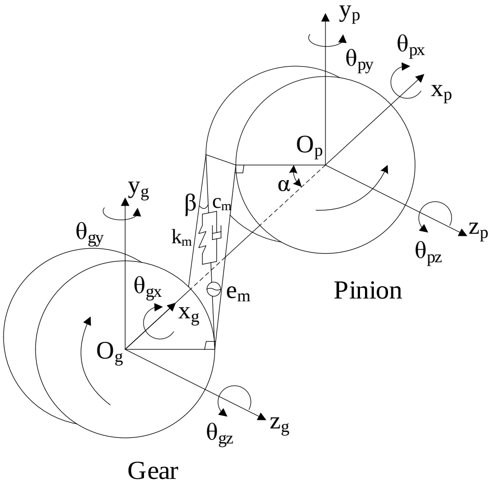

Figure 2. 12 DOF dynamic model of a helical gear pair

$$M_P\ddot{x}_p + k_m\delta \times \frac{\partial \delta}{\partial x_p} + c_m\dot{\delta} \times \frac{\partial \dot{\delta}}{\partial \dot{x}_p} = (k_m e_m + c_m \dot{e}_m)\sin\alpha\cos\beta \tag{2}$$

$$M_P\ddot{y}_p + k_m\delta \times \frac{\partial \delta}{\partial y_p} + c_m\dot{\delta} \times \frac{\partial \dot{\delta}}{\partial \dot{y}_p} = (k_m e_m + c_m \dot{e}_m)\cos\alpha\cos\beta \tag{3}$$

$$M_P\ddot{z}_p + k_m\delta \times \frac{\partial \delta}{\partial z_p} + c_m\dot{\delta} \times \frac{\partial \dot{\delta}}{\partial \dot{z}_p} = -(k_m e_m + c_m \dot{e}_m)\sin\beta \tag{4}$$

$$I_{px}\ddot{\theta}_{px} + k_m\delta \times \frac{\partial \delta}{\partial \theta_{px}} + c_m\dot{\delta} \times \frac{\partial \dot{\delta}}{\partial \dot{\theta}_{px}} = 0 \tag{5}$$

$$I_{py}\ddot{\theta}_{py} + k_m\delta \times \frac{\partial \delta}{\partial \theta_{py}} + c_m\dot{\delta} \times \frac{\partial \dot{\delta}}{\partial \dot{\theta}_{py}} = -(k_m e_m + c_m \dot{e}_m)\sin\beta \times R_p \tag{6}$$

$$I_{pz}\ddot{\theta}_{pz} + k_m\delta \times \frac{\partial \delta}{\partial \theta_{pz}} + c_m\dot{\delta} \times \frac{\partial \dot{\delta}}{\partial \dot{\theta}_{pz}} = -(k_m e_m + c_m \dot{e}_m)\sin\beta \times r_p \tag{7}$$

$$M_g\ddot{x}_g + k_m\delta \times \frac{\partial \delta}{\partial x_g} + c_m\dot{\delta} \times \frac{\partial \dot{\delta}}{\partial \dot{x}_g} = -(k_m e_m + c_m \dot{e}_m)\sin\alpha\cos\beta \tag{8}$$

$$M_g\ddot{y}_g + k_m\delta \times \frac{\partial \delta}{\partial y_g} + c_m\dot{\delta} \times \frac{\partial \dot{\delta}}{\partial \dot{y}_g} = -(k_m e_m + c_m \dot{e}_m)\cos\alpha\cos\beta \tag{9}$$

$$M_g\ddot{z}_g + k_m\delta \times \frac{\partial \delta}{\partial z_g} + c_m\dot{\delta} \times \frac{\partial \dot{\delta}}{\partial \dot{z}_g} = (k_m e_m + c_m \dot{e}_m)\sin\beta \tag{10}$$

$$I_{gx}\ddot{\theta}_{gx} + k_m\delta \times \frac{\partial \delta}{\partial \theta_{gx}} + c_m\dot{\delta} \times \frac{\partial \dot{\delta}}{\partial \dot{\theta}_{gx}} = 0 \tag{11}$$

$$I_{gy}\ddot{\theta}_{gy} + k_m\delta \times \frac{\partial \delta}{\partial \theta_{gy}} + c_m\dot{\delta} \times \frac{\partial \dot{\delta}}{\partial \dot{\theta}_{gy}} = -(k_m e_m + c_m \dot{e}_m)\sin\beta \times R_g \tag{12}$$

$$I_{gz}\ddot{\theta}_{gz} + k_m\delta \times \frac{\partial \delta}{\partial \theta_{gz}} + c_m\dot{\delta} \times \frac{\partial \dot{\delta}}{\partial \dot{\theta}_{gz}} = -(k_m e_m + c_m \dot{e}_m)\,sin\,\beta \times r_g \tag{13}$$

where, M_p and M_g presents the mass of gear pairs, I_p and I_g their moment of inertia in each direction,$r_p$and r_g shows their base radius. R_p and R_g reveals their pitch radius while δ is for their total deformation in meshing direction. In the above Eqs. (1-13), the relative displacement of gear mesh in a direction perpendicular to teeth contact surfaces is defined as:

$$\delta = \begin{Bmatrix} (-x_p + x_g)\sin\alpha + \\ (y_p - y_g)\cos\alpha + (-r_p\theta_{pz} + r_g\theta_{pz}) \end{Bmatrix} \cos\beta + \begin{Bmatrix} (-z_p + z_g) + \\ (-R_p\theta_{py} + R_g\theta_{gy}) \end{Bmatrix} \sin\beta \tag{14}$$

Shaft Element Analysis

To study the influence of shaft deformation on transmission dynamics characteristics in transmission dynamics model, the shaft is considered as an elastic body. After applying Lagrange's equations, the equation of motion for the shaft is defined below while the mass matrix, gyro matrix, damping matrix and stiffness matrix are based on [19].

$$M^e\{\ddot{q}^e\} + \{\Omega G^e + C^e\}\{\dot{q}^e\} + K^e\{q^e\} = 0 \tag{15}$$

Bearing Element Analysis

Generally, each shaft is supported by two radial element bearings with varying types and parameters. Furthermore, they are modeled in terms of stiffness and the damping matrices. The equation of motion for bearing elements will be:

$$C^b\{\dot{q}^b\} + K^b\{q^b\} = 0 \tag{16}$$

where,

$$K^b = \begin{bmatrix} k_{xx} & k_{xy} & k_{xz} & k_{x\theta x} & k_{x\theta y} \\ k_{yx} & k_{yy} & k_{yz} & k_{y\theta x} & k_{y\theta y} \\ k_{zx} & k_{zy} & k_{zz} & k_{z\theta x} & k_{z\theta y} \\ k_{\theta xx} & k_{\theta xy} & k_{\theta xz} & k_{\theta x\theta x} & k_{\theta x\theta y} \\ k_{\theta yx} & k_{\theta yy} & k_{\theta yz} & k_{\theta y\theta x} & k_{\theta y\theta y} \end{bmatrix}$$

and,

$$C^b = \begin{bmatrix} C_{xx} & C_{xy} & C_{xz} & C_{x\theta x} & C_{x\theta y} \\ C_{yx} & C_{yy} & C_{yz} & C_{y\theta x} & C_{y\theta y} \\ C_{zx} & C_{zy} & C_{zz} & C_{z\theta x} & C_{z\theta y} \\ C_{\theta xx} & C_{\theta xy} & C_{\theta xz} & C_{\theta x\theta x} & C_{\theta x\theta y} \\ C_{\theta yx} & C_{\theta yy} & C_{\theta yz} & C_{\theta y\theta x} & C_{\theta y\theta y} \end{bmatrix}$$

Overall System

Every subsystem is developed by using the finite element method to get the combined equation of the single stage-helical gear transmission system. By combining all the previous equations:

$$M^s\{\ddot{q}^s\} + \{\Omega G^s + C^s\}\{\dot{q}^s\} + K^s\{q^s\} = F^s \tag{17}$$

In the formula, M^s, G^s, C^s, K^s, F^s are systems mass matrix, gyroscopic matrix, damping matrix, stiffness and force matrix respectively while q^s is the node displacement matrix. However, the mass and gyroscopic contributions to the global matrices are imagined the same in this section as those of lumped disks at the nodes of the gear pairs in rotor dynamics models and thus, are not be emphasized in this piece of work. Figure 3 shows combined finite element model comprised of variety of 12 nodes located at different positions of input and output shaft.

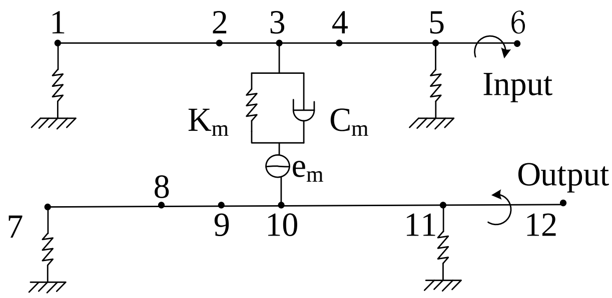

Figure 3. Finite element model for overall system

NUMERICAL ANALYSIS AND DISCUSSION

Based on the modeling method in previous part, the stiffness, damping and mass matrix of bearing element, gear meshing element and shaft element are calculated according to the basic parameters of the gear system shown below.

Table 1. Bearing parameters for stiffness

Stiffness	Barings	k_{xx}	k_{yy}	k_{zz}	$k_{\theta x \theta x}$	$k_{\theta y \theta y}$
Bearing 1	SFK:16004	2.18×10^{08}	2.41×10^{08}	2.30×10^{07}	1.02×10^{10}	1.03×10^{10}
Bearing 2	SFK:16004	2.40×10^{08}	2.34×10^{08}	4.88×10^{07}	1.64×10^{10}	1.67×10^{10}
Bearing 3	QJ6204	2.55×10^{08}	1.00×10^{09}	3.32×10^{07}	1.10×10^{06}	1.20×10^{06}
Bearing 4	NSK:16004	4.47×10^{08}	8.26×10^{08}	3.16×10^{07}	1.00×10^{06}	1.00×10^{06}

Table 2. Geometric parameters for gear pair

Parameter	Unit	Value
Number of teeth on pinion	-	19
Number of teeth on gear	-	87
Normal module	(mm)	2
Pressure angle	(α)	14.5°
Helix angle	(β)	30°
Centre distance	(mm)	125
Input torque	(N.m)	96
Output torque	(N.m)	438.3

The whole dynamic model of the gear system is established according to the dynamic equation of the system. Finally, we used the numerical solution method to solve the dynamic equation. Using the Newmark -beta method, acceleration response in Figure 4(a) and 4(b) is calculated for input shaft speed of 3000 rev/min and 9000 rev/min at node 3 where the left bearing is located on driving shaft.

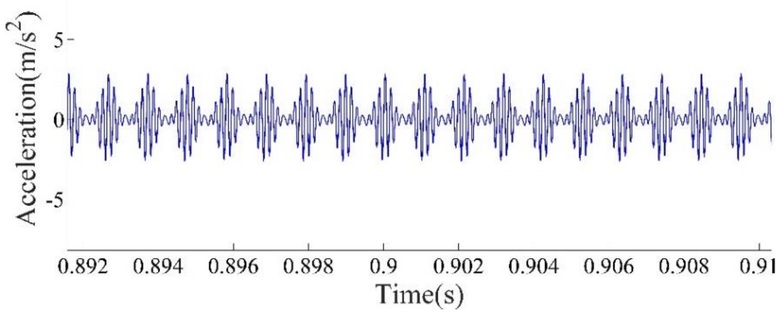

(a)

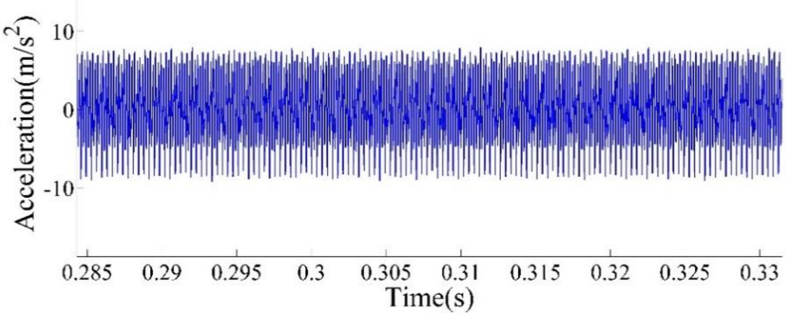

(b)

Figure 4. Vibration acceleration for different rotational speeds at node 3: (a) 3000 rev/min and (b) 9000 rev/min

Figure 5 shows the peak-peak acceleration response for different speeds at node 1 in x, y and z directions. Higher acceleration can be seen for y and z direction for a speed of 6500 rev/min which is critical, while in x-direction, over-all acceleration is minimum as compared to y and z direction but still maximum acceleration is obvious for a speed of 6500 rev/min in x-direction.

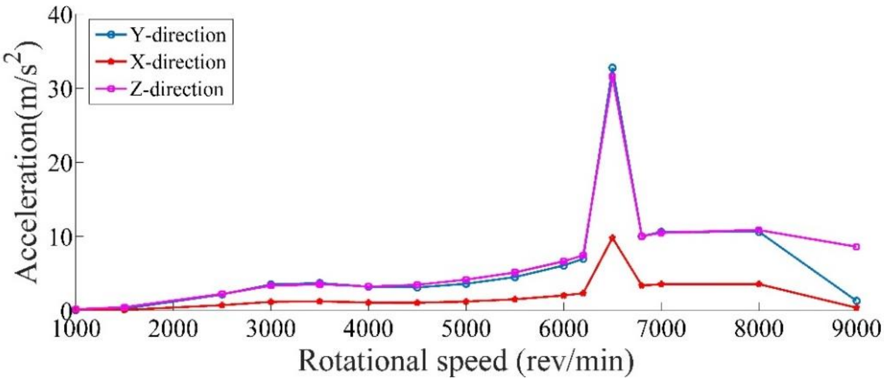

Figure 5. Acceleration response map along X, Y and Z-direction at Node 1 for different speeds

To demonstrate the meshing force effects on gear dynamics, mesh force is analyzed for different loads of single stage helical gear bearing system. The gear mesh force that varies with time, give rise to the vibrations. In Figure 6, as the input shaft rotational speed gets higher, the mesh fluctuation goes higher but the highest fluctuation can be seen at speed = 6500rev/min. It is noticeable that for a speed of 7000 rev/min and 8000rev/min, fluctuation level is not that high as compared to critical speed of 6500 rev/min. So, it can be deduced that reduction of the vibration of gear system is achievable by avoiding the critical speed and reducing the mesh force.

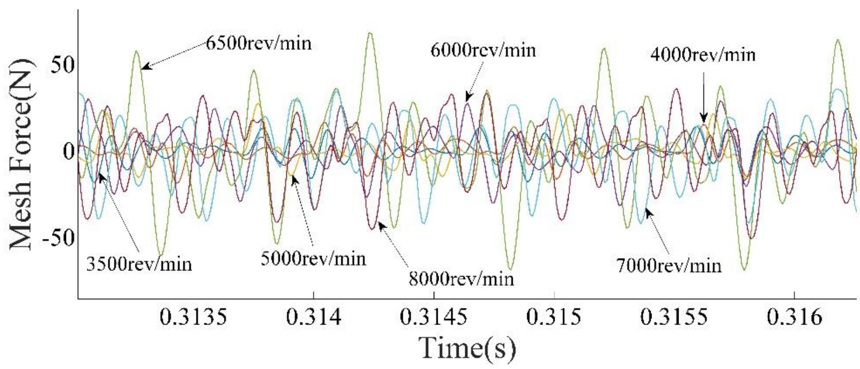

Figure 6. Mesh force vs time for different load and rotational speed

Figure 7 explains the relation between driving shaft rotational speed and peak to peak mesh force. It is interesting that maximum peak to peak value can be seen for a rotational speed of 6500 rev/min. But generally, it's obvious that as the speed is getting higher, mesh force is going to increase. But after critical speed of 6500 rev/min, peak to peak mesh force is not high even for rotational speed of 7000 rev/min and 8000 rev/min. As the rotational speed increases above this level, the mesh force decreases in magnitude. The reason for using the higher load is based on the assumption that a higher load and speed will result in a higher variation in the transmission error and thus result in more severe vibrations. In contrast, here 6500 rev/min can be seen as worst-case critical speed condition for the transmission, with respect to gear noise and vibration.

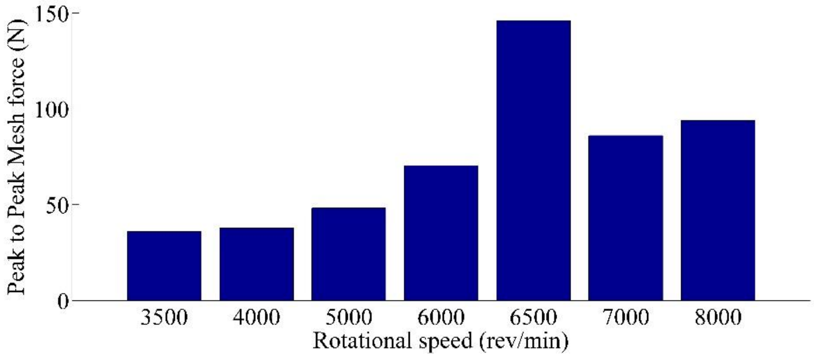

Figure 7. Peak to peak mesh force vurses rotational speed

Figure 8(a) depicts the transmission error variations with varying applied speeds. It is noticeable that the transmission error variation is inferior for the low speed of 3500 rev/minute and goes higher with the increasing speed. In addition, the increase in variation of transmission error is not linear with the variation in speed. A similar trend can be seen for the peak to peak mesh force variation for different speeds in Figure 7. Since the mesh force of a given gear pair rely on several parameters, particularly the rotational speed of the supported shafts so again the most significant peak for the mesh force can be seen for the critical speed of 6500 rev/minute in Figure 6.

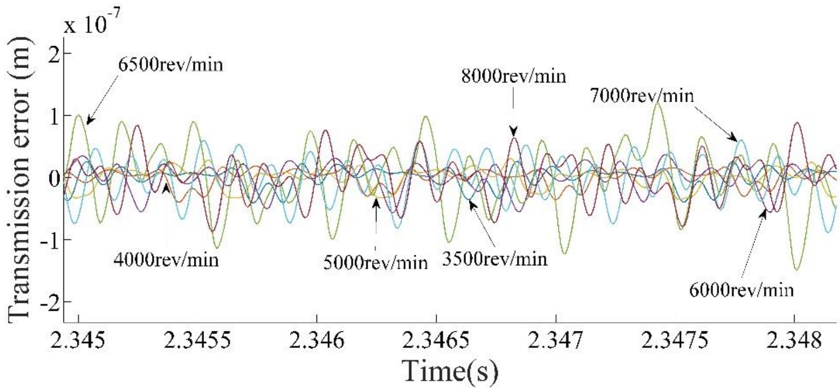

Figure 8(a). Transmission error vs time for different load and speed

As the speed varies and goes down, transmission error goes in the similar trend. By comparing the transmission error in Figure 8(b), it is obvious that transmission error decreases for lower operating speed (3500 rev/minute). Very little impact on the transmission error at lower speed ranges can be seen in Figure 8(a) and (b).

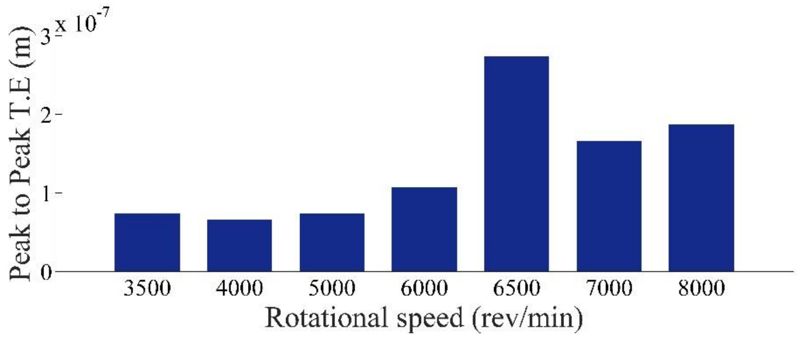

Figure 8(b). Peak to peak transmission error vs rotational speed

To find the driving force behind critical speed and to check the validity of prescribed model, MASTA was used to analyze the single stage helical gear system with the same parameters as shown in Table 1 and 2.

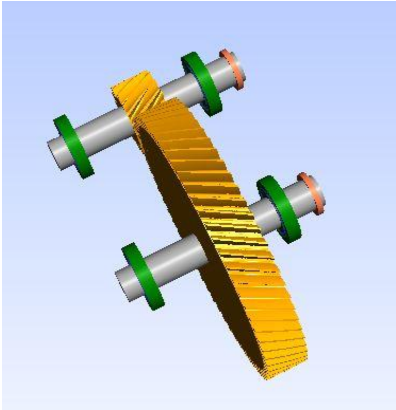

(a)

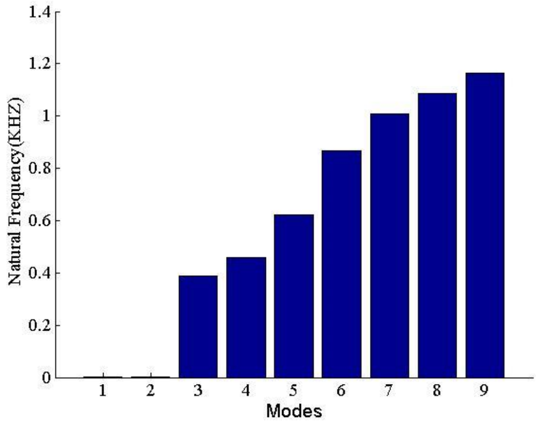

(b)

Figure 9. (a) MASTA 3-D model and (b) damped natural frequencies

Figure 9(a) and 9(b) shows the three-dimensional model in MASTA and its natural frequencies for first 9 harmonics. In addition, the geared system is made from a material with a Young's modulus of 2.054 x 10^{11} N/m, Poisson's ratio of 0.32 and a density of 7750 kgm^{-3}. Using free boundaries, quadratic tetrahedral cells were meshed. For *inertial properties,* the location, mass, polar, and diametric moment of inertia were specified. Then, bearing properties were ignored for simplicity and same gyroscopic terms mentioned earlier were applied. As a result of the stability analysis, the damped natural frequency of the geared system was obtained. Each line represents a frequency evolution with respect to increased rotational speeds and possible resonant condition is highlighted for a specific vibration mode. Figure 10 describes potential resonant point which occurs for a speed of almost 6500 rev/minute and natural frequency 0.45 kHz where the mesh harmonics intersect with natural frequencies. By looking deep into details of the Figure 10, it is obvious that the change in dynamic characteristic for 6500 rev/minute and appearance of resonance occur due to gyroscopic effect and natural frequencies of the system. This mechanism further leads to dramatic rise in the transmission error as well as vibration level of the gear system at critical speed. By comparing Figures 9(b) and 10, it is also apparent that 4th order mode is the dangerous vibration mode of the over-all geared system in this study which causes critical speed at 0.45 kHz.

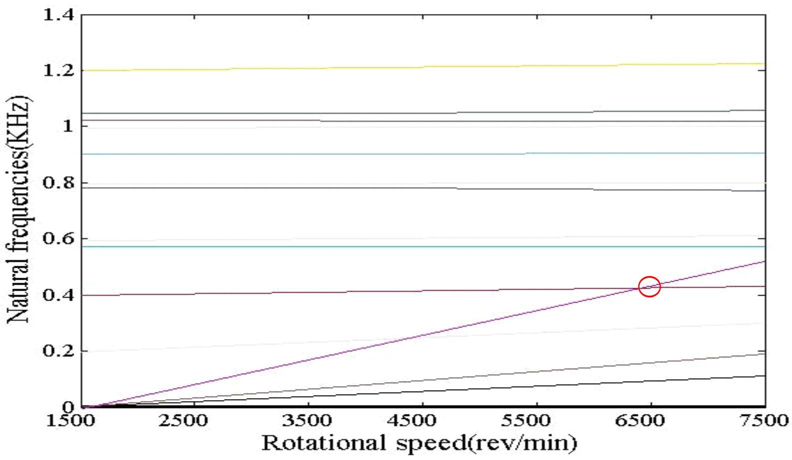

Figure 10. Comparison of natural frequencies and rotational speeds

CONCLUSIONS

A full dynamic model of the bearing, shaft element and the gear meshing of the proposed system is established by using the finite element method and the lumped parameter. Based on the idea of finite element modeling, the mass matrix, stiffness matrix and damping matrix of the equations of the three subsystem models are assembled. Newmark-βeta method was used to solve the dynamic equations and some of the influence factors of dynamic response on the system such as the critical speed is gained which came out to be 6500 rev/minute. In addition, acceleration response map for different speeds is analyzed. Then the stability analysis was performed using MASTA to know the dynamics behind the critical speed. By analyzing Campbell diagram, it was concluded that the natural frequency corresponding to 0.45 kHz have a huge impact which may even lead to worsen the dynamic response in operating conditions so to avoid the critical speed and its consequences, natural frequencies are equally important to be considered regarding vibration reduction for helical gear systems. When the input speed goes higher, the dynamic mesh force becomes large, so the amplitude of vibration acceleration follows upward trend obviously. However, there is a turning point due to the critical speed of 6500 rev/min, which further leads to rise in both mesh force and transmission error. Therefore, it is inferred that critical speed during operating conditions should be avoided which can enhance not only the dynamic mesh force but also can cause severe vibrations as a result of transmission error.

ACKNOWLEDGEMENTS

The authors would like to thank to the Chongqing University for laboratory facilities to carry out this research.

REFERENCES

[1] H. Nevzat Özgüven, and D. R. Houser, “Mathematical models used in gear dynamics—A review,” *Journal of Sound and Vibration*, vol. 121, no. 3, pp. 383–411, 1988.

[2] G.W. Blankenship, and R. Singh, A comparative study of selected gear mesh interface dynamic models. Advancing power transmission into the 21st century. 137-46, 1992.

[3] S.V. Neriya, R.B. Bhat, and T.S. Sankar, “Coupled torsional-flexural vibration of a geared shaft system using finite element analysis,” The Shock and Vibration Bulletin, 1985.

[4] A. Kahraman, H. Ozguven, and D. Houser, “Dynamic analysis of geared rotors by finite elements,” 1992.

[5] H.N. Özgüven, “A non-linear mathematical model for dynamic analysis of spur gears including shaft and bearing dynamics,” *Journal of Sound and Vibration*, vol. 145, no. 2, pp. 239-60, 1991.

[6] M. Maatar and P. Velex, “Quasi-static and dynamic analysis of narrow-faced helical gears with profile and lead modifications,” 1997.

[7] S.V. Neriya, R.B. Bhat, and T.S. Sankar, Coupled torsional-flexural vibration of a geared shaft system using finite element analysis. The Shock and Vibration Bulletin, 1985.

[8] A. Kahraman, “Effect of axial vibrations on the dynamics of a helical gear pair,” 1993.

[9] J. A. Kaplan, S. Dousti, P. E. Allaire, B. R. Nichols, T. W. Dimond, and A. Untaroiu, “Rotor dynamic modeling of gears and geared systems,” in Proceedings of the ASME Turbo Expo, vol. 7A, 2013.

[10] B. Giorgio, and F. Pellicano, "Non-smooth dynamics of spur gears with manufacturing errors," *Journal of Sound and Vibration*, vol. 306, no. 1-2, pp. 271-283, 2007.

[11] K. Woohyung, H. H. Yoo, and J. Chung, "Dynamic analysis for a pair of spur gears with translational motion due to bearing deformation," *Journal of Sound and Vibration*, vol. 329, no. 21, pp. 4409-4421, 2010.

[12] C.H. Kang, et al., "Dynamic analysis of gear-rotor system with viscoelastic supports under residual shaft bow effect," *Mechanism and Machine Theory*, vol. 46, no. 3, pp. 264-275, 2011.

[13] M. Rui, Y. Chen, and Q. Cao, "Research on dynamics and fault mechanism of spur gear pair with spalling defect," *Journal of Sound and Vibration*, vol. 331, no. 9, pp. 2097-2109, 2012.

[14] M. Hamed, and H. Salarieh, "Analysis of nonlinear oscillations in spur gear pairs with approximated modelling of backlash nonlinearity," *Mechanism and Machine Theory*, vol. 51, pp. 14-31, 2012.

[15] H. Ma, J. Yang, R. Song, S. Zhang, and B. Wen, “Effects of tip relief on vibration responses of a geared rotor system,” *Proc. Inst. Mech. Eng. Part C, J. Mech. Eng. Sci.*, vol. 228, no. 7, pp. 1132–1154, 2014.

[16] H. Qinkai, and F. Chu, "Dynamic behaviors of a geared rotor system under time-periodic base angular motions," *Mechanism and Machine Theory*, vol. 78, pp. 1-14, 2014.

[17] M. Inalpolat, M. Handschuh, and A. Kahraman, "Influence of indexing errors on dynamic response of spur gear pairs," *Mechanical Systems and Signal Processing*, vol. 60, pp. 391-405, 2015.

[18] Mohammed, Omar D., Matti Rantatalo, and Jan-Olov Aidanpää, "Dynamic modelling of a one-stage spur gear system and vibration-based tooth crack detection analysis," *Mechanical Systems and Signal Processing*, vol. 54, pp. 293-305, 2015.

[19] C. Siyu, et al., "Rotordynamics analysis of a double-helical gear transmission system," *Meccanica*, vol. 51, no. 1, pp. 251-268, 2016.

[20] Z. Hu, J. Tang, S. Chen, and D. Lei, “Effect of mesh stiffness on the dynamic response of face gear transmission system,” *J. Mech. Des. Trans. ASME*, vol. 135, no. 7, 2013.

[21] L. Zhai, Y. Luo, Z. Wang, S. Kitauchi, and K. Miyagawa, “Nonlinear vibration induced by the water-film whirl and whip in a sliding bearing rotor system,” *Chinese J. Mech. Eng. (English Ed.)*, vol. 29, no. 2, pp. 260–270, 2016.

[22] A. Jahanbakhshi, B. Ghamari, and K. Heidarbeigi, “Vibrations analysis of combine harvester seat in time and frequency domain,” *J. Mech. Eng. Sci.*, vol. 14, no. 1, pp. 6251–6258, 2020.

[23] M. F. Isham, M. S. Leong, L. M. Hee, and Z. A. B. Ahmad, “Iterative variational mode decomposition and extreme learning machine for gearbox diagnosis based on vibration signals,” *J. Mech. Eng. Sci.*, vol. 13, no. 1, pp. 4477–4492, 2019.